Available online at www.sciencedirect.com
ScienceDirect
Scripta Materialia 58 (2008) 850–853
Scripta MATERIALIA
www.elsevier.com/locate/scriptamat

Athermal grain growth through cooperative migration of grain boundaries in deformed nanomaterials

M.Yu. Gutkin,* K.N. Mikaelyan and I.A. Ovid'ko

Institute of Problems of Mechanical Engineering, Russian Academy of Sciences, Bolshoj 61, Vasilievskii Ostrov, St. Petersburg 199178, Russia

Received 10 December 2007; revised 2 January 2008; accepted 2 January 2008
Available online 11 January 2008

A special mode of both athermal grain growth and associated plastic deformation in nanocrystalline metals and ceramics is theoretically described. The mode represents the stress-induced cooperative migration of grain boundaries when the migration involves two or more neighboring boundaries. We calculated two critical external stress levels attributed to the start of migration of two neighboring boundaries and their meeting, respectively. After their convergence, grain boundaries can annihilate, stop, move together or move in opposite directions, depending on their characteristics.

Keywords: Grain growth; Grain-boundary migration; Plastic deformation; Nanocrystalline materials; Disclinations

The extraordinary mechanical properties of nanocrystalline (nc) materials are strongly influenced by specific grain-boundary-mediated mechanisms of plasticity [1–5]. In recent years, special attention has been paid to one of these mechanisms, namely stress-induced grain growth. Many experiments have demonstrated that it occurs during plastic deformation in ultrafine-grained (ufg) and nc metals and alloys at room [6–16] and cryogenic [9,10] temperatures. Stress-induced grain growth and elongation have been observed in superplastic ufg [17–19] and nc [20] ceramics at high temperatures. Although the basic micromechanisms of low-temperature stress-induced grain growth in nc/ufg metals and high-temperature strain-induced grain elongation in nc/ufg ceramics may be different, one expects some common features in these phenomena.

Recent computer simulations [21–27] have shown that low-temperature stress-induced grain growth in nc metals is athermal. Its basic mechanisms are found to be stress-induced migration of grain boundaries (GBs) and their triple junctions, GB sliding, grain rotation and coalescence. Also, stress-induced GB migration and athermal grain growth have been described theoretically with the aid of two-dimensional (2-D) dislocation–disclination models [28–31]. These models predict the existence of critical stresses for migration of low- and high-angle GBs. However, the models [28–31] are focused on only sole GBs. At the same time, stress-induced migration often involves two or more neighboring GBs that may converge, and this cooperative migration is significantly different from migration of a sole GB. The main aim of this paper is to theoretically describe collective migration of two interacting GBs as a special mode of both athermal grain growth and associated plastic deformation in nc materials.

Consider a model 2-D arrangement of rectangular grains G1–G3, with G1/G2 and G2/G3 being two low-angle tilt GBs, finite walls of perfect lattice dislocations characterized by the tilt misorientation parameters Ω and ω (Fig. 1a and b). In the initial state, these GBs form four triple junctions which are supposed to be geometrically balanced (the sum of GB misorientation angles at each of these junctions is equal to zero). Under an external shear stress τ, athermal migration of GBs from their initial positions A and D to new positions B and C occurs. As a result, the angle gaps $\pm\Omega$ and $\pm\omega$ appear at the double junctions at A and D, and four new triple junctions with the angle gaps $\pm\Omega$ and $\pm\omega$ are formed at B and C, respectively. Straight line defects (double junctions at A and D, and triple junctions at B and C) characterized by the angle gaps $\pm\Omega$ and $\pm\omega$ are partial wedge disclinations whose motion produces rotational plastic deformation [32]. Thus, stress-induced migration of the low-angle tilt GBs G1/G2 and G2/G3 carries plastic deformation and results in the formation

* Corresponding author. E-mail: gutkin@def.ipme.ru

1359-6462/$ - see front matter
doi:10.1016/j.scriptamat.2008.01.002

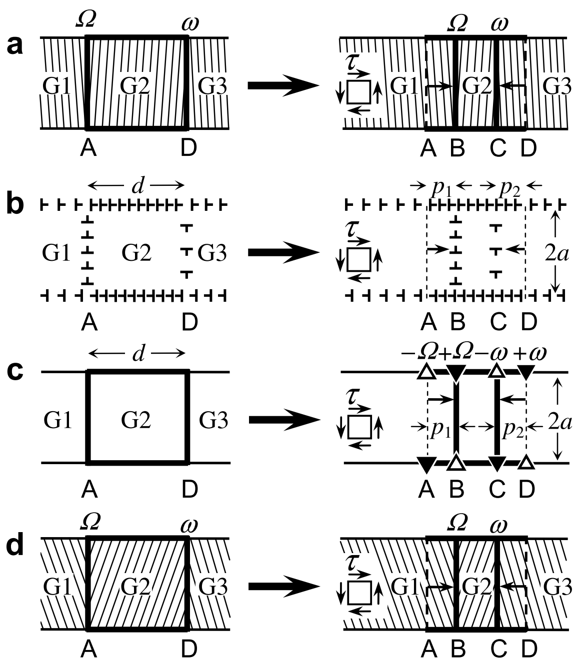

Figure 1. Geometric (a, d), dislocation (b) and disclination (c) models for stress-induced cooperative migration of two low-angle (a, b) or high-angle (c, d) grain boundaries under an external shear stress τ.

of four two-axis dipoles of partial wedge disclinations (Fig. 1c): two Ω-dipoles (A and B) and two ω-dipoles (C and D). The same is true for migration of two high-angle tilt GBs with large Ω and ω (Fig. 1c and d).

Our 2-D model does not include factors relevant to real nc materials, such as the general type and finite size of GBs, their distribution in size and misorientation, or the strong influence of impurities [7,8,16,33] and applied stress gradient [6–10,12,33] on dislocation glide and GB migration. Nevertheless, it allows us to discern new essential features in collective GB migration.

Let us analyze the energy of the system during its evolution. When the disclination structure appears as a result of the GB migration (Fig. 1c), the total energy of the system drastically changes. Following Refs. [32,34], we find the energy change ΔW (per unit of the disclination length) as

$$\begin{aligned}\Delta W = 2Da^2\Omega^2\{&(x^2+1)\ln(x^2+1) - x^2\ln x^2 \\ &+ \lambda^2[(y^2+1)\ln(y^2+1) - y^2\ln y^2] \\ &+ \lambda\{(z^2+1)\ln(z^2+1) - z^2\ln z^2 \\ &+ [(z-x-y)^2+1]\ln[(z-x-y)^2+1] \\ &- (z-x-y)^2\ln(z-x-y)^2 \\ &- [(z-x)^2+1]\ln[(z-x)^2+1] \\ &+ (z-x)^2\ln(z-x)^2 \\ &- [(z-y)^2+1]\ln[(z-y)^2+1] \\ &+ (z-y)^2\ln(z-y)^2\} - \frac{2\tau}{D\Omega}(x+\lambda y)\}, \end{aligned} \tag{1}$$

where $D = G/[2\pi(1-\nu)]$, G is the shear modulus, ν is the Poisson ratio, $2a$ is the arm of a disclination dipole (A, B, C or D), $x = p_1/2a, y = p_2/2a, z = d/2a$ and $\lambda = \omega/\Omega$. Here p_1 and p_2 are the distances passed by the migrated GBs G1/G2 and G2/G3, respectively, and d is the initial size (length) of grain G2.

Since ΔW depends upon two variables, x and y, it is convenient to study its behavior with contour maps $\Delta W(x,y) = \text{const}$ (due to the restrictions of space, we do not show them here). They enable one to examine some characteristic features of the system's evolution. In particular, we analyzed local minima of the function $\Delta W(x,y)$ (Fig. 2a and c) and the most probable trajectories along the maximum gradient of ΔW (Fig. 2b and d) of the system's development in the space (x,y). Let us first consider the case of an initially equiaxed $(z = 1)$ grain G2 with $\lambda = 1$. If the external stress τ is small (here $\tau < 0.3D\Omega$), ΔW is always positive and the GB migration is impossible. When τ becomes larger than some critical level τ_c, ΔW is negative at small x and y, reaching a minimum, with coordinates x and y determining the stable equilibrium positions of migrating GBs B (G1/G2) and C (G2/G3). These equilibrium positions are marked by open circles in Figure 2a, where the dashed arrow shows the general direction of the system's evolution from one equilibrium state to another. The insets schematically demonstrate the stable equilibrium states of the GB arrangement under a given value of τ. Due to the anti-symmetry of the disclination model in the case where $\lambda = 1$, the equilibrium points lie at the bisectrix 1–4. In other words, GBs B and C synchronously migrate to each other (see insets 1–4) under increasing τ.

Using Eq. (1), one can estimate τ_c as follows. Let $x = y$, $z = 1$, $\lambda = 1$ and $x \ll 1$. Then Eq. (1) results in $\Delta W \approx -2Dd^2\Omega^2 x(x + x\ln x + \tau/D\Omega)$. Elementary migration of a GB by an interatomic distance b is possible if $\Delta W(x = b/d) < 0$. Therefore, the equation $\Delta W(x = b/d) = 0$ gives the critical stress τ_c:

$$\tau_c \approx \frac{D\Omega b}{d}\left(\ln\frac{d}{b} - 1\right) \tag{2}$$

If we omit the unit in the brackets, we obtain formula (3) in Ref. [31], which estimates the critical stress τ_{c1} for the migration of a sole GB. More careful examination of the model from Ref. [31] gives $\tau_{c1} \approx D\Omega(b/d)[\ln(d/b) + 1]$, and hence the difference $\Delta\tau_c = \tau_{c1} - \tau_c \approx 3D\Omega b/(2d)$ reflects the effect of elastic interaction of migrating GBs on the critical stress. It is evident that $\Delta\tau_c \sim d^{-1}$. Let us estimate τ_c and $\Delta\tau_c$ for nc metal (Al) and ceramic (β-Si_3N_4) with typical values $\Omega = 0.085(\approx 5^\circ)$ and $d = 100$ nm. For Al with $G = 27$ GPa, $\nu = 0.31$ and $b \approx 0.25$ nm, we get $\tau_c \approx 7$ MPa and $\Delta\tau_c \approx 2$ MPa. For β-Si_3N_4, we use the elastic moduli measured at 1375° C [35]: $G \approx 128$ GPa and $\nu = 0.32$. The hexagonal lattice parameters are $a \approx 0.76$ nm and $c \approx 0.29$ nm [35]. Therefore, we take $b = a$ for GB migration in the a-direction (the a-case) and $b = c$ for GB migration in the c-direction (the c-case). As a result, in the a-case, $\tau_c \approx 75$ MPa and $\Delta\tau_c \approx 29$ MPa. In the c-case, $\tau_c \approx 36$ MPa and $\Delta\tau_c \approx 11$ MPa. These values of τ_c are easily achievable in real experiments on tension of nc Al [14,15] and compression [20] and tension [35] of β-Si_3N_4. When the external stress τ achieves another characteristic value τ_m, GBs B and C meet and can annihilate or pass through each other. This stress value is determined from

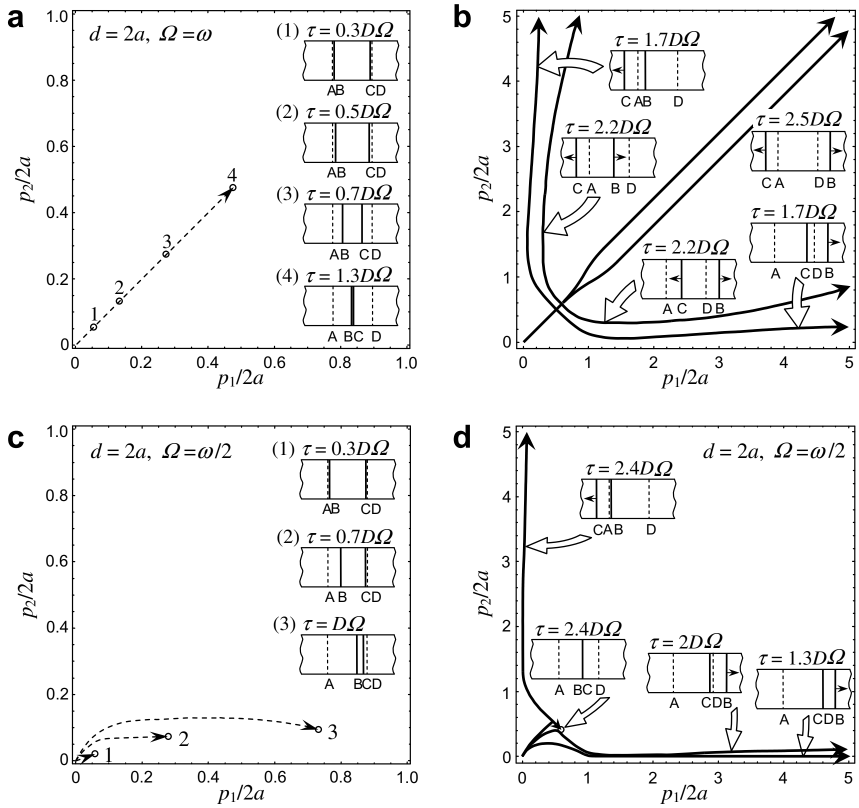

Figure 2. Diagrams of cooperative migration of two opposite grain boundaries in the space of their normalized displacements ($x = p_1/2a$, $y = p_2/2a$) under different levels of the external shear stress τ at $\lambda = 1$ (a, b) and $\lambda = 2$ (c, d). Plots (a) and (c) show stable equilibrium positions 1–4 of the grain boundaries. Plots (b) and (d) demonstrate trajectories of unstable GB migration. The insets image the initial (A and D) and equilibrium or unstable (B and C) positions of migrating grain boundaries.

the condition of minimum for $\Delta W(x,y)$ at $x = y$, $z = 1$, $\lambda = 1$ and $x = 1/2$ (the meeting point): $\partial\Delta W/\partial x = 2Dd^2\Omega^2(\ln 5 - \tau_m/D\Omega) = 0$, which gives $\tau_m = D\Omega \ln 5 \approx 1.6D\Omega$. It is interesting that, first, this result does not depend on the grain size d, and, second, it is twice as high as the second critical stress, $\tau_{c2} \approx 0.8D\omega$, for the unstable migration of a sole GB [31]. For the same values of parameters, taken for nc Al and nc β-Si_3N_4, we obtain the following estimates: $\tau_m \approx 0.85$ and 4.1 GPa, respectively. In the case of nc Al, this value is in accordance with the level of local ($\leqslant$1.4 GPa) [25] and even overall ($\approx$0.8 GPa) [27] shear stresses in computer simulations of nanoindentation [25] and tension [27] of pure nc Al, where migration of low-angle GBs and the growth of one grain at the expense of another were observed. In the case of nc β-Si_3N_4, our estimate ($\tau_m \approx$ 4.1 GPa) is $\approx$6 times smaller than the shear stress level found in a computer simulation of shear deformation of single-crystal β-Si_3N_4 at room temperature [36], but greatly exceeds the experimentally measured flow stress in nc Si_3N_4-based ceramic [20], in which strain-induced elongation (by a factor $\approx$3) of grains occurs in the course of superplastic deformation at high temperatures. The discrepancy between our estimate and experimental data [20] can be related to the effects of high-temperature diffusion causing intensive relaxation of disclination stresses, thereby decreasing the value of τ_m in superplastic nc Si_3N_4-based ceramic [20]. In other words, both athermal (stress-induced) and thermally activated processes contribute to GB migration in this nc ceramic.

If $\tau \geqslant \tau_m$, a point of bifurcation appears (Fig. 2b). This may be treated as follows: the migrating GBs B and C do not annihilate but pass through each other. This is possible, for instance, if GBs are low-angle (dislocation walls) and the glide planes of dislocations from the opposite GBs do not coincide. The bifurcation point is a result of our assumption that $\lambda = 1$. Indeed, in this case there is no difference between these GBs, and two equivalent situations are possible: (i) GB B passes through GB C and captures it (see the bottom right curve in Fig. 2b). The leading GB B and the trailing GB C migrate together until GB B reaches position D ($x = 1$) and continues into grain G3. GB C stays in its equilibrium position near point D ($y \approx 0.2$ at $\tau = 1.7D\Omega$). When τ grows enough (here at $\tau = 2.2D\Omega$), GB C begins to migrate back to point A (the coordinate y gradually increases, and the corresponding curve in Fig. 2b declines up); finally, GB C passes through point A into grain G1. As a result, grains G1 and G3 are unified in one grain with the lattice orientation as in pre-existed grain G2. If τ is very large (here $\tau = 2.5D\Omega$), GBs B and C pass through each other and continue their migration with the same final result as in the previous case (see the bottom straight arrow in Fig. 2b). (ii) This case is the exact opposite: GB C passes through GB B and capture it (see the left curve in Fig. 2b), etc. The scenario is the same as in case (i) with the changes $B \leftrightarrow C$, $A \leftrightarrow D$, $x \leftrightarrow y$ and $G1 \leftrightarrow G3$. The same final result may be considered as unstable growth of grain G2 at the expense of grains G1 and G3.

Consider now the case $\lambda = 2$ (Fig. 2c and d). As can be seen, there is no symmetry in GB migration in this case. GB B (having a lower misorientation parameter) migrates by a larger equilibrium distance than GB C under a stress level $\tau \geqslant \tau_c$ (Fig. 2c). Therefore, to estimate τ_c, one can ignore the shift of GB C that gives $\tau_c \approx \tau_{c1} \approx D\Omega(b/d)[\ln(d/b) + 1]$, a result obtained above for a sole GB. A further increase in τ breaks the stability of the GB migration. At $\tau = 1.3D\Omega \approx \tau_m$, GB B reaches GB C and annihilates or passes through it and captures it (see the bottom curve in Fig. 2d). They then migrate together to point D, where GB B leaves GB C and migrates into the bulk of grain G3, while GB C occupies its initial position at point D. If τ is larger (here at $\tau = 2D\Omega$), the situation is similar, but GB C first reaches point D and then migrates back to point A. At the next stress level (here at $\tau = 2.4D\Omega$), the point where GBs meet becomes a point of bifurcation: GBs B and C can coalesce and remain at an equilibrium point (here $x \approx 0.57$, $y \approx 0.43$), shown by the open circle in Figure 2d, or GB C captures GB B and they migrate together to point A, where GB C leaves GB B and migrates into the bulk of grain G1, while GB B rests near point A. When τ grows further, both the bifurcation and equilibrium points disappear, and the last situation is repeated.

In summary, we have considered stress-induced cooperative GB migration as a special mode of both athermal grain growth and associated plastic deformation in nc metals and ceramics. We have shown that two critical stresses, τ_c and τ_m, control the behavior of migrating GBs. When the external shear stress τ reaches τ_c, opposite GBs start to migrate to each other, their migration is stable and their equilibrium positions are determined by $\tau \geqslant \tau_c$. When $\tau \geqslant \tau_m \gg \tau_c$, the GBs meet. Then the following regimes of cooperative migration are possible at $\tau > \tau_m$, depending on τ level and GB characteristics: (i) GBs are annihilated when their misorientations are equal in magnitude but opposite in sign; (ii) one GB captures another GB and they migrate together in one direction under a moderate τ; (iii) GBs coalesce and remain at a local equilibrium position; or (iv) GBs can overcome their mutual attraction and migrate in opposite directions under a very large τ. In all cases, GB migration leads to the unstable growth of a grain at the expense of its neighbors.

The work was supported, in part, by the Office of US Naval Research (Grant N00014-07-1-0295), the Russian Federal Agency of Science and Innovations (Contract 02.513.11.3190), the National Science Foundation Grant CMMI #0700272, and CRDF (Grant RUE2-2684-ST-05).

[1] K.S. Kumar, H. Van Swygenhoven, S. Suresh, Acta Mater. 51 (2003) 5743.
[2] M.Yu. Gutkin, I.A. Ovid'ko, Plastic Deformation in Nanocrystalline Materials, Springer, Berlin, 2004.
[3] D. Wolf, V. Yamakov, S.R. Phillpot, A.K. Mukherjee, H. Gleiter, Acta Mater. 53 (2005) 1.
[4] M. Dao, L. Lu, R.J. Asaro, J.T.M. De Hosson, E. Ma, Acta Mater. 55 (2007) 4041.
[5] C.C. Koch, I.A. Ovid'ko, S. Seal, S. Veprek, Structural Nanocrystalline Materials: Fundamentals and Applications, Cambridge University Press, Cambridge, 2007.
[6] M. Jin, A.M. Minor, E.A. Stach, J.W. Morris Jr., Acta Mater. 52 (2004) 5381.
[7] W.A. Soer, J.Th.M. De Hosson, A.M. Minor, J.W. Morris Jr., E.A. Stach, Acta Mater. 52 (2004) 5783.
[8] J.T.M. De Hosson, W.A. Soer, A.M. Minor, Z. Shan, E.A. Stach, S.A. Syed Asif, O.L. Warren, J. Mater. Sci. 41 (2006) 7704.
[9] K. Zhang, J.R. Weertman, J.A. Eastman, Appl. Phys. Lett. 85 (2004) 5197;
K. Zhang, J.R. Weertman, J.A. Eastman, Appl. Phys. Lett. 87 (2005) 061921.
[10] P.L. Gai, K. Zhang, J. Weertman, Scripta Mater. 56 (2007) 25.
[11] X.Z. Liao, A.R. Kilmametov, R.Z. Valiev, H. Gao, X. Li, A.K. Mukherjee, J.F. Bingert, Y.T. Zhu, Appl. Phys. Lett. 88 (2006) 021909.
[12] D. Pan, T.G. Nieh, M.W. Chen, Appl. Phys. Lett. 88 (2006) 161922.
[13] D. Pan, S. Kuwano, T. Fujita, M.W. Chen, Nano Lett. 7 (2007) 2108.
[14] D.S. Gianola, S. Van Petegem, M. Legros, S. Brandstetter, H. Van Swygenhoven, K.J. Hemker, Acta Mater. 54 (2006) 2253.
[15] D.S. Gianola, D.H. Warner, J.F. Molinari, K.J. Hemker, Scripta Mater. 55 (2006) 649.
[16] G.J. Fan, L.F. Fu, H. Choo, P.K. Liaw, N.D. Browning, Acta Mater. 54 (2006) 4781.
[17] F. Wakai, H. Kato, Adv. Ceram. Mater. 3 (1988) 71.
[18] N. Kondo, F. Wakai, T. Nishioka, A. Yamakawa, J. Mater. Sci. Lett. 14 (1995) 1369.
[19] N. Kondo, E. Sato, F. Wakai, J. Amer. Ceram. Soc. 81 (1998) 3221.
[20] X. Xu, T. Nishimura, N. Hirosaki, R.-J. Xie, Y. Yamamoto, H. Tanaka, Acta Mater. 54 (2006) 255.
[21] A. Hasnaoui, H. Van Swygenhoven, P.M. Derlet, Acta Mater. 50 (2002) 3927.
[22] J. Schiøtz, Mater. Sci. Eng. A 375–377 (2004) 975.
[23] D. Farkas, A. Frøseth, H. Van Swygenhoven, Scripta Mater. 55 (2006) 695.
[24] J. Monk, D. Farkas, Phys. Rev. B 75 (2007) 045414.
[25] F. Sansoz, V. Dupont, Appl. Phys. Lett. 89 (2006) 111901.
[26] F. Sansoz, J.F. Molinari, Thin Solid Films 515 (2007) 3158.
[27] T. Shimokawa, A. Nakatani, H. Kitagawa, Phys. Rev. B 71 (2005) 224110.
[28] S.V. Bobylev, M.Yu. Gutkin, I.A. Ovid'ko, Acta Mater. 52 (2004) 3793.
[29] S.V. Bobylev, M.Yu. Gutkin, I.A. Ovid'ko, Phys. Solid State 46 (2004) 2053.
[30] J.C.M. Li, Phys. Rev. Lett. 96 (2006) 215506.
[31] M.Yu. Gutkin, I.A. Ovid'ko, Appl. Phys. Lett. 87 (2005) 251916.
[32] A.E. Romanov, V.I. Vladimirov, in: F.R.N. Nabarro (Ed.), Dislocations in Solids, vol. 9, North Holland, Amsterdam, 1992, pp. 191–402.
[33] W.A. Soer, J.Th.M. De Hosson, A.M. Minor, Z. Shan, S.A. Syed Asif, O.L. Warren, Appl. Phys. Lett. 90 (2007) 181924.
[34] M.Yu. Gutkin, K.N. Mikaelyan, A.E. Romanov, P. Klimanek, Phys. Stat. Sol. (a) 193 (2002) 35.
[35] G.A. Swift, E. Üstühdag, B. Clausen, M.A.M. Bourke, H.-T. Lin, Appl. Phys. Lett. 82 (2003) 1039.
[36] S. Ogata, H. Kitagawa, N. Hirosaki, Y. Hatanaka, T. Umezu, Comp. Mater. Sci. 23 (2002) 146.